Docking of novel reversible monoamine oxidase-B inhibitors: Efficient prediction of ligand binding sites and estimation of inhibitors thermodynamic properties

ARTICLE *in* JOURNAL OF NEURAL TRANSMISSION · JUNE 2007

Impact Factor: 2.4 · DOI: 10.1007/s00702-007-0679-7 · Source: PubMed

3 AUTHORS, INCLUDING:

Kemal Yelekçi
Kadir Has University
25 PUBLICATIONS **305** CITATIONS

SEE PROFILE

J Neural Transm (2007)
DOI 10.1007/s00702-007-0679-7
Printed in The Netherlands

Journal of Neural Transmission

Docking of novel reversible monoamine oxidase-B inhibitors: efficient prediction of ligand binding sites and estimation of inhibitors thermodynamic properties

K. Yelekçi[1], Ö. Karahan[2], M. Toprakçı[3]

[1] The Faculty of Arts and Sciences, Kadir Has University, Fatih-Istanbul, Turkey
[2] Chemistry Department, Faculty of Arts and Sciences, Bogazici University, Istanbul, Turkey
[3] Department of Biochemistry, The School of Medicine, Istanbul Bilim University, Istanbul, Turkey

Received: September 3, 2006 / Accepted: December 17, 2006 / Published online: March 31, 2007

Summary Monoamine oxidase (MAO, EC 1.4.3.4) is a flavoenzyme bound to the mitochondrial outer membranes of the cells, which is responsible for the oxidative deamination of neurotransmitter and dietary amines. It has two distinct isozymic forms, designated MAO-A and MAO-B, each displaying different substrate and inhibitor specificities. They are the well-known target for antidepressant, Parkinson's disease and neuroprotective drugs. Elucidation of the x-ray crystallographic structure of MAO-B has opened the way for molecular modeling studies. In this research 12 reversible and MAO-B selective inhibitors have been docked computationally to the active site of the MAO-B enzyme. AutoDock 3.0.5 was employed to perform the automated molecular docking. The result of docking studies generated thermodynamic properties, such as free energy of bindings (ΔG_b) and inhibition constants (K_i) for the inhibitors. Moreover, 3D pictures of inhibitor-enzyme complexes afforded valuable data regarding the binding orientation of each inhibitor in the active site of MAO-B.

Keywords: Docking calculations, reversible MAO-B inhibitors, three dimentional picture of inhibitor-enzyme complex

Abbreviations

MAO monoamine oxidase
PM3 parameterized model number 3

Introduction

Monoamine oxidase (MAO, EC 1.4.3.4) is a flavoenzyme bound to the mitochondrial outer membrane of the cell, which is responsible for the oxidative deamination of neurotransmitter and dietary amines (Hubalek et al., 2003; Bach et al., 1998; Youdim et al., 2006). Two isozymes of MAO, namely A and B, have been identified on the basis of their substrate preference and inhibitor selectivity. Inhibitors of MAO-A are clinically used as antidepressants and anxiolytics (Pare, 1976; Shih et al., 1999), while MAO-B inhibitors are used for the treatment of Parkinson's disease and for symptoms associated with Alzheimer's disease (Binda et al., 2004; Terud and Langston, 1989). Recent studies have demonstrated that the irreversible MAO-B inhibitor rasagiline (*N*-propargyl-1*R*-aminoindan) has neuroprotective activity in neuronal cells (Youdim et al., 2005). A considerable amount of work has accumulated in the past few years with the goal of elucidating the oxidation mechanism of MAO. The major breakthrough has been brought about by the crystallization of the human MAO-B with several different irreversible MAO-B inhibitors (Binda et al., 2002, 2004; De Colibus et al., 2005).

Determination of the 3D structure of MAO-B facilitated the development of computer-assisted more selective and reversible MAO-B inhibitor design. So far we have carried out some preliminary modeling studies (Erdem and Yelekci, 2001; Toprakci and Yelekci, 2005; Yelekci and Silverman, 1998; Erdem et al., 2006), as have others (Carotti et al., 2002; Carrieri et al., 2002; Manna et al., 2002; Veselovsky et al., 2004; Li et al., 2006), in order to gain insights into the molecular factors affecting MAO inhibition activity and selectivity. As an extension of our previous studies on docking a series of experimentally tested MAO-B inhibitors, here we report the docking of 12 reversible MAO-B selective inhibitors, selected from the

Correspondence: Kemal Yelekçi, The Faculty of Arts and Sciences, Kadir Has University, 34231 Fatih-Istanbul, Turkey
e-mail: yelekci@khas.edu.tr

Table 1. *Names and structures of the selected, reversible MAO-B inhibitors*

Names	Structures
1-(Aminomethyl)cyclopropanebenzylcarboxylate (**1**)	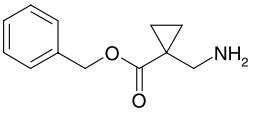
N,N-dimethylbenzylamine (**2**)	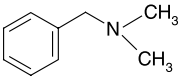
Cinnamylamine-2,3-oxide (**3**)	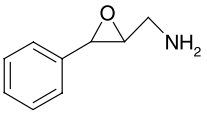
5-[4-(4-Methoxybenzyloxy)phenyl]-2-(2-cyanoethyl)-1,3,4-oxadiazol-2(3H)-thione (**4**)	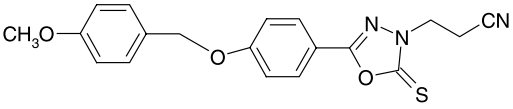
trans,*trans*-Farnesol (**5**)	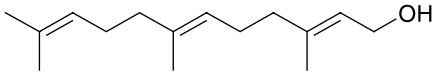
N-(2-Cyanoethyl)-N-ethylcarboxy-4-benzyloxyphenylhydrazone (**6**)	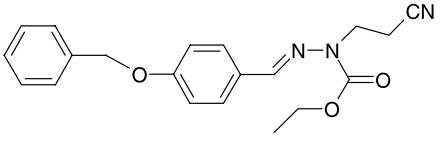
N-(2-Aminoethyl)-p-chlorobenzamid (**7**)	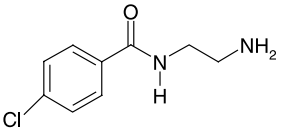
5-(4-Biphenylyl)-3-(2-cyanoethyl)-1,3,4-oxadiazol-2 (3H) thione (**8**)	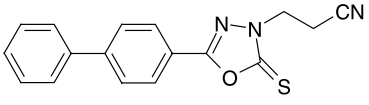
5-(4-Biphenylyl)-3-(2-cyanoethyl)-1,3,4-oxadiazol 2(3H)-one (**9**)	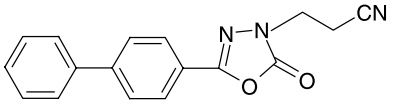
5-[4-(Benzyloxy)phenyl]-2-(2-cyanoethyl)-1,3,4-oxadiazol-2(3H)-one (**10**)	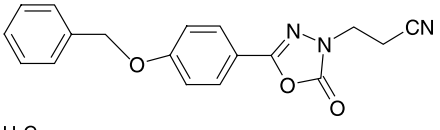
(+)-(R)-1-Thiocarbamoyl-3-(4-methylphenyl)-5-(4-chlorophenyl)-4,5-dihydro-(1H)-pyrazole (**11**)	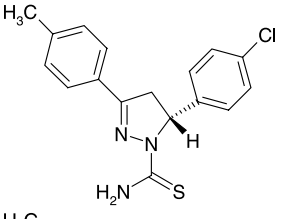
(−)-(S)-1-Thiocarbamoyl-3-(4-methylphenyl)-5-(4-chlorophenyl)-4,5-dihydro-(1H)-pyrazole (**12**)	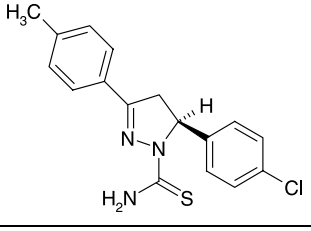

literature, with varying inhibition constants (K_i) and structural features (Table 1) The docking studies results generated inhibitor thermodynamic properties, such as free energy of binding (ΔG) and K_i values. Moreover, 3D pictures of inhibitor-enzyme complexes afforded invaluable data regarding the binding orientation of inhibitors in on the active site of MAO-B.

Methods

Protein setup

The high-resolution crystal structure of monoamine oxidase-B, co-crystalized with its irreversible inhibitor 6-hydroxy-*N*-propargyl-1(*R*)-aminoindan, was obtained from the Protein Data Bank (PDB entry code 1S3E, 1.6 Å resolution) (http://www.rcsb.org). The study was carried out on only one subunit of the enzyme protein. The pdb file was edited and the β-chain was removed together with an irreversible inhibitor of MAO-B, the 6-hydroxy-*N*-propargyl-1(*R*)-aminoindan group. Additionally side-chain optimization in the active region only was also performed. This treatment optimized the 1E3S structure further and the conformational changes resulting from binding of the original inhibitor in the crystal structure were partially removed.

In order to use the protein in the Autodock docking simulation program, all polar hydrogens were added with the GROMACS modeling package (Berendsen et al., 1995; Lindahl et al., 2001). The structure obtained was optimized in 400 steps of conjugate gradient minimization, employing the GROMOS-87 force field. During minimization the heavy atoms were kept fixed at their initial crystal coordinates, but added hydrogens were made free to move. Minimization was performed under a vacuum medium. Electrostatic interactions were calculated using the cut-off method. After the acceptable minimal force gradient was reached, the resultant protein structure was saved. Finally atomic solvation parameters of protein and FAD were assigned using the ADDSOL utility of AutoDock 3.0.5.

Ligands

For docking experiments with AutoDock 3.0.5 (Morris et al., 1998, 1999), the 3D structures of ligand molecules were built, optimized – PM3 level), and saved in mol2 format with the aid of the molecular modeling program Spartan (Wavefunction Inc.) and VEGA programs (Pedretti et al., 2004). All hydrogens were added. Partial atomic charges were also calculated by the Gasteiger–Marsili method (Gasteiger and Marsili, 1980) using the VEGA program, and saved in pdbq format. All possible flexible torsions of the resultant ligand molecules were defined by using AUTOTORS 3.05 auxiliary program.

Docking

AutoDock 3.0.5 was employed to perform a docking simulation using a Lamarckian genetic algorithm (Morris et al., 1998). The standard docking procedure for rigid protein and flexible ligands whose torsion angles were identified was used for 10 independent runs per ligand. The grid maps were calculated using Autogrid (version 3.06), one of the utility programs of Autodock. In all docking a grid of 60, 60, 60 points in x, y, and z directions was built and, because the location of the inhibitor in the complex was known, the maps were centered on the N5 atom of the flavin (FAD) in the catalytic site of the protein. A grid spacing of 0.375 Å (approximately one forth of the length of carbon–carbon covalent bond) and a distances-dependent function of the dielectric constant were used for the calculation of the energetic map. The default settings were used for all other parameters. At the end of docking, ligands with the most favorable free energy of binding were selected as the resultant complex structures. All calculations were carried out on PC based machines running Linux x86 as operating systems. The resultant structure files were analyzed using VMD (Humphrey et al., 1996) (Visual Molecular Dynamics) visualization programs.

Results

Reversible and selective MAO-B inhibitors (**1**–**12**) with varying structural features and inhibition constants were selected from the literature and were docked into the catalytic site of MAO-B (Table 1). The results of LGA docking experiments with these inhibitors are summarized in Table 2. The estimated free energy of binding (ΔG_b), calculated inhibition constants (K_i) as well as experimental inhibition constants for each enzyme-inhibitor complex are shown.

Figure 1, panels 1–4, show the docked models of compound **1**–**4**. Contrary to most of the docking modes, the model for compound **1** shows the benzyl moiety is not stacked between Tyr398 and Tyr435. The cyclopropyl group is vertically inserted between these two side chains and the carboxylate group is much closer to the Tyr435 side

Table 2. *AutoDock estimated free energies of binding (ΔG_b), calculated [K_i (calculated)] and experimental [K_i (experimental)] inhibition constants of the inhibitors studied (temperature = 298.15 K)*

Inhibitors	ΔG_b (kcal/mol) (calculated)	K_i (μM) (calculated)	K_i (μM) (experimental)	Reference
1	−6.54	16.0	200	Silverman et al. (1997)
2	−6.30	24.0	151	Edmondson et al. (2000)
3	−6.78	10.7	110	Silverman et al. (1994)
4	−5.30	131	14.3	Leberton et al. (1995)
5	−9.0	0.251	2.3	Hubalek et al. (2005)
6	−7.86	1.72	1.32	Carrieri et al. (2002)
7	−8.31	0.804	0.142	Cesura et al. (1996)
8	−11.43	4.19×10^{-3}	40×10^{-3}	Mazouz et al. (1990)
9	−11.33	4.98×10^{-3}	26×10^{-3}	Mazouz et al. (1990)
10	−10.40	23.7×10^{-3}	6.93×10^{-3}	Leberton et al. (1995)
11	−11.32	5.04×10^{-3}	$2.7\ (\pm 0.07) \times 10^{-3}$	Chimenti et al. (2005)
12	−11.68	2.74×10^{-3}	$1.0\ (\pm 0.07) \times 10^{-3}$	Chimenti et al. (2005)

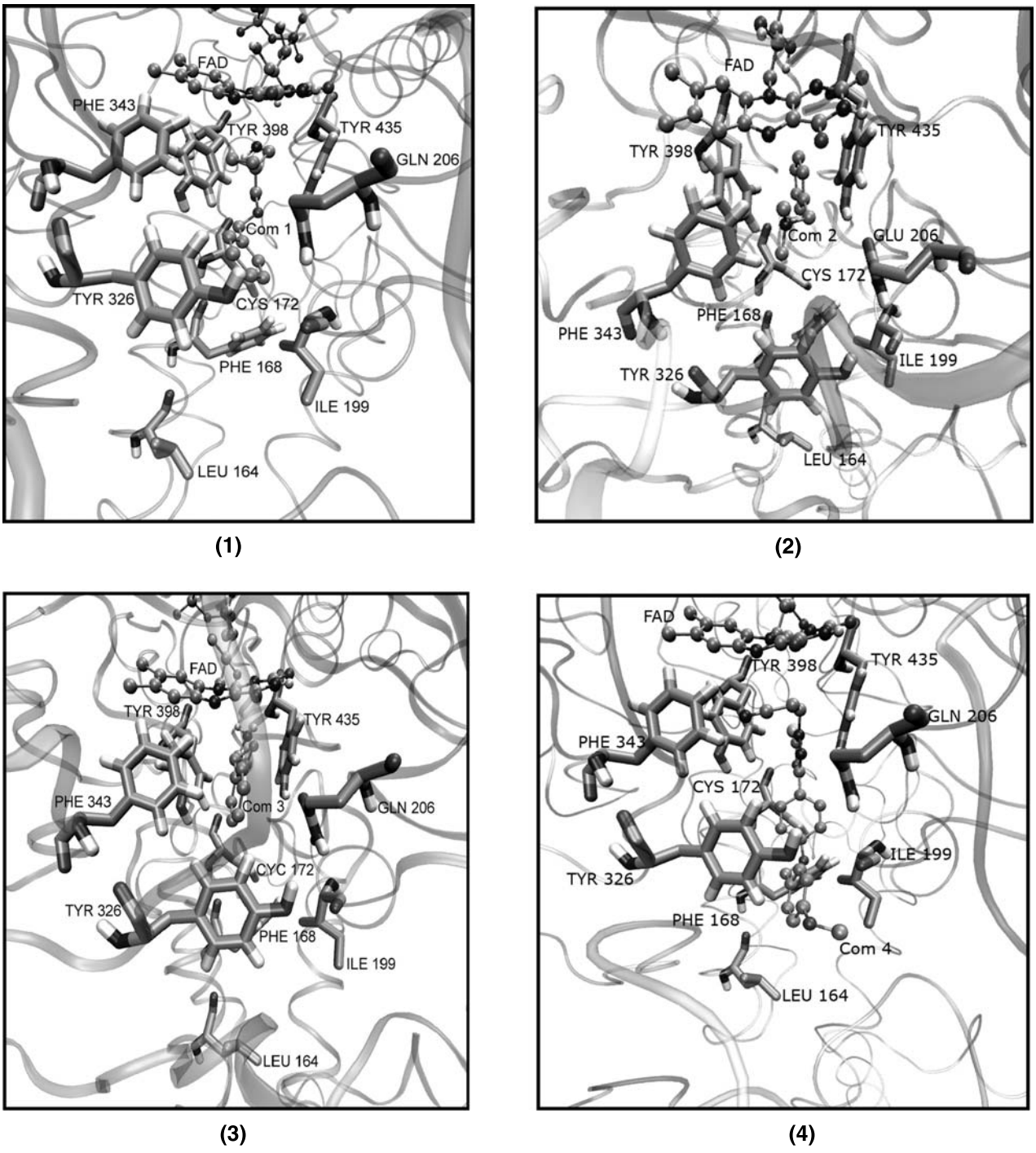

Fig. 1. Docking result of compounds **1**, **2**, **3**, **4** with MAO-B. The inhibitors and FAD were designated in CPK style, the important residues in the active site of the enzyme were presented by ligorice style. Part of the enzyme in the background was visualized in New Ribbon style using the VMD program

chain than Tyr398. The amino moiety is aligned to the N5 atom of FAD as closely as possible (a distance of 3.61 Å). The other favorable interaction is between the phenolic hydroxyl of Tyr435 and the etheric oxygen of the inhibitor (2.58 Å). In the binding of inhibitor **2** within the enzyme cavity, the benzyl group is sandwiched between Tyr398 and Tyr435. However the phenyl ring is closer (3.18 Å) to the Tyr398 than Tyr435 (3.71 Å). For compound **3**, the phenyl ring is located far from both Tyr398 and Tyr435 and the oxirane ring approaches the FAD, from *re* face, as closely as possible. The distance between the oxirane ring oxygen and the C4 atom of FAD is 2.98 Å. The other close distance

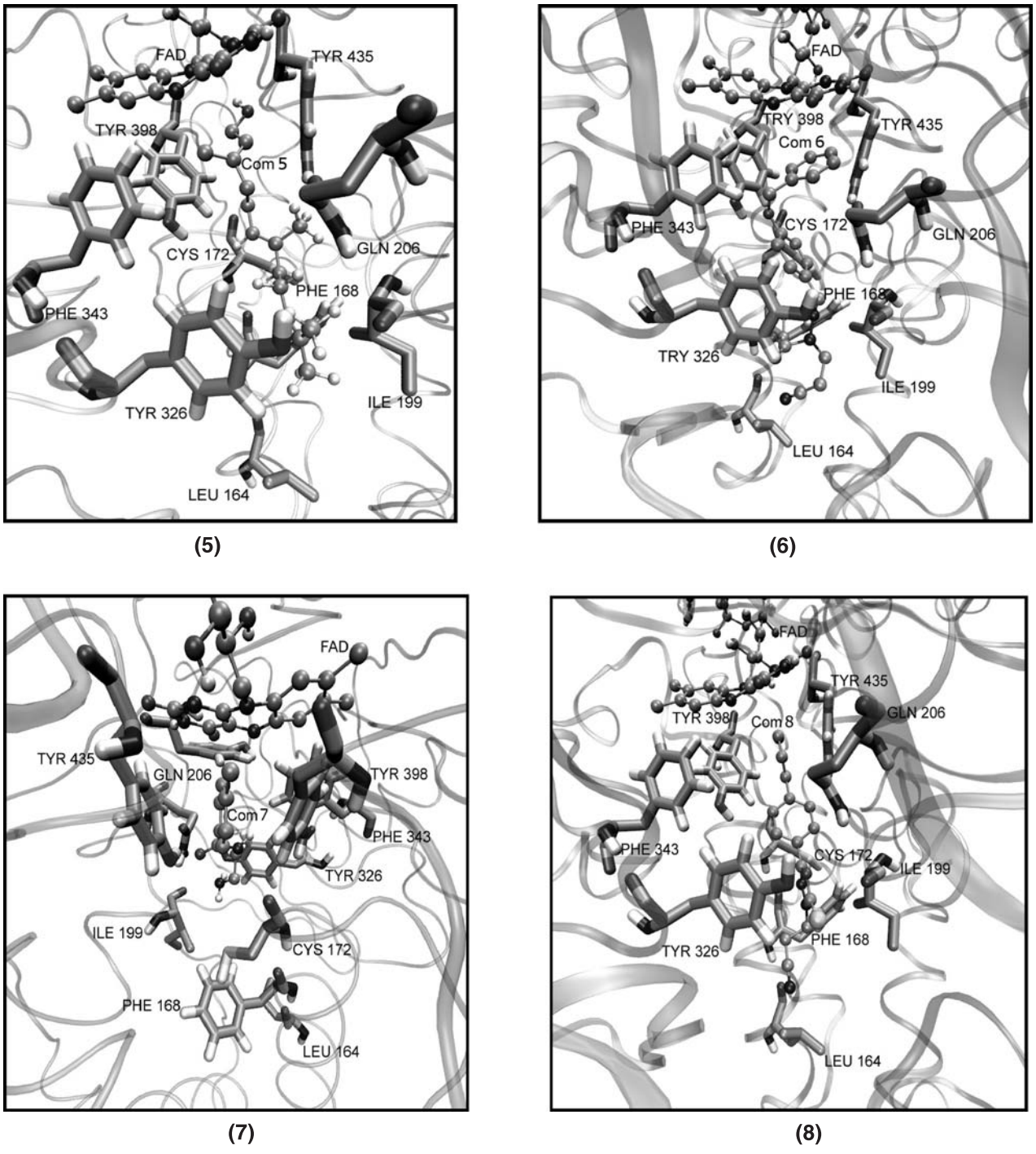

Fig. 2. The interacting mode of compounds **5**, **6**, **7**, **8** with MAO-B. The important residues of the enzyme and the inhibitors are depicted by ligorice and CPK model, respectively

is between the amino moiety of this compound and the N5 atom of the FAD (3.79 Å). In the binding mode of the compound **4**, it is interesting to see that the 1, 3, 4-oxadiazol-2(3H)-thione moiety is in close proximity with Tyr435.

Figure 2, panels 5–8, show the docked models of compounds **5**–**8**. With compound **5** the hydroxyl tail is inserted between Tyr398 and Tyr435. The isopropyl terminal extends toward the entrance cavity and makes close contact with the Ile199 side chain. In the docked mode of compound **6**, the benzoyloxy group is fitted between the Tyr398 and Tyr435 side chains. The distance between the benzoyl oxygen and the hydroxyl group of Tyr398 is about 2.73 Å.

Phe168, Leu164 and Ile199 residues nicely surrounded the cyanoethyl moiety of the compound.

The optimal binding mode of compound **7** in the active site of the enzyme shows that the amine moiety adopts a position in the vicinity of the *re* face of FAD cofactor and the chlorobenzamide part is positioned between two tyrosyl residues, 398 and 435. Moreover there is one important hydrogen bond (a distance of 1.90 Å) between the carbonyl group and hydroxyl group of the Tyr435. In the binding mode of compound **8**, the benzyl group is stacked between Tyr398 and Tyr435. The benzoyloxy oxygen molecule is positioned at a distance of 2.22 Å, nearer to the Tyr435 hydroxy group than the Tyr398 hydroxy group (a distance of 5.31 Å). The oxadiazine ring is positioned in a volume surrounded by Ile199, Cys172, Phe168, and Leu164 and the cyanoethyl group extends toward the entrance cavity.

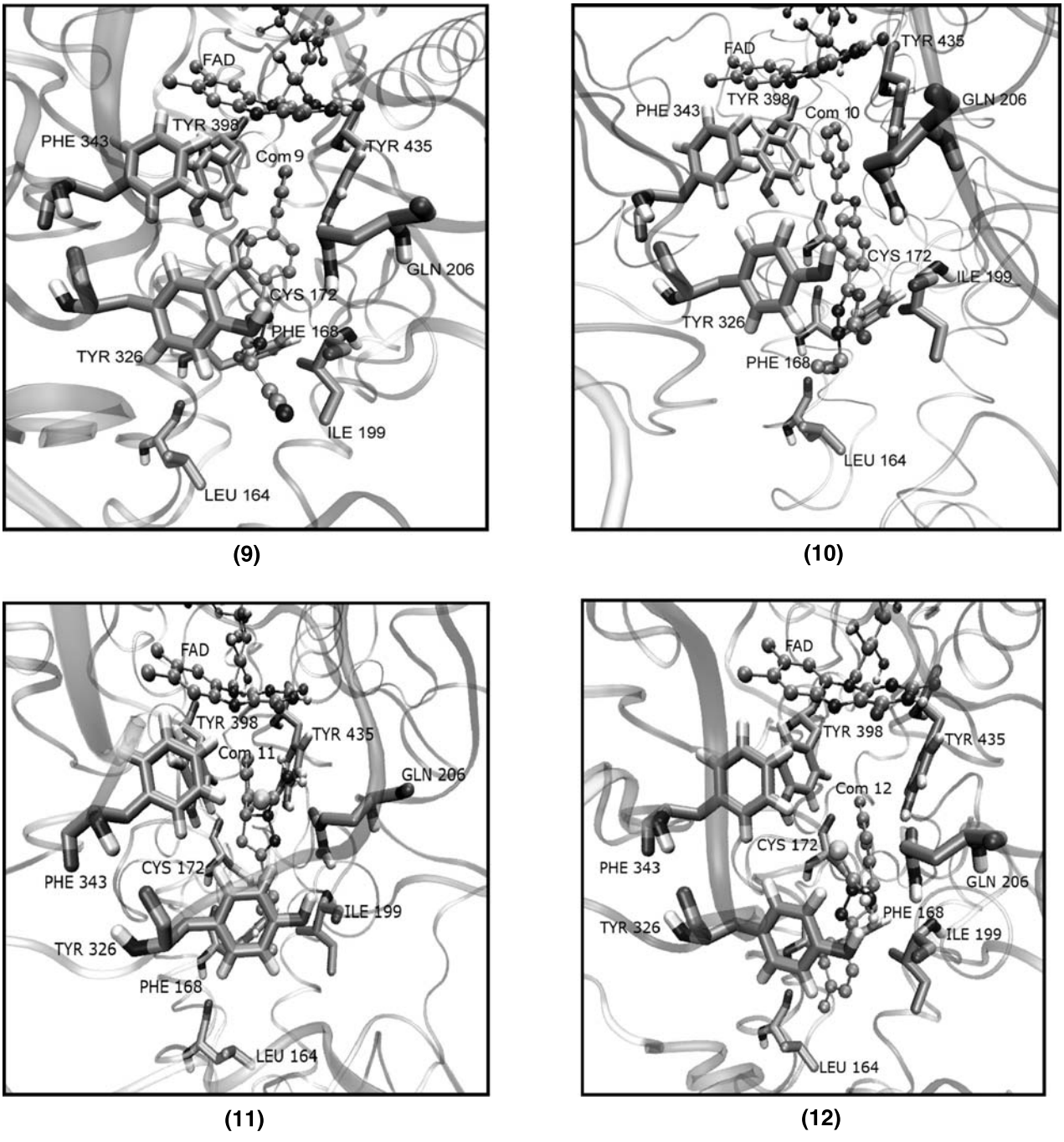

Fig. 3. The interacting mode of compounds **9**, **10**, **11**, **12** and their orientations in the active site of the enzyme

Figure 3, panels 9–12, show the docked models of compounds **9**–**12**. Careful evaluation of the binding pocket revealed that compounds **9** and **10** adopt the same binding mode; their phenyl rings are sandwiched in between Tyr398 and Tyr435 and their cyanoethyl groups are aligned along the entrance cavity. Varying degrees of electrostatic and van der Waals interactions with the residues of Cys172, Gln206, Ph168, and Ile199 may contribute to the binding and stabilization of these compounds in the entrance cavity space.

In contrast to most of the previous docking modes, no phenyl ring stacking behavior was observed between Tyr398 and Tyr435 in the docking model for (+)-*R*-thiocarbomyl-3-(4-methylphenyl)-5-(4-chlorophenyl)-4,5-dihydro-(1H)-pyrazole (compound **11**). This agrees with the results of Chimenti et al. (2005). However, the Cl atom on the phenyl ring has van der Waals contacts with isoalloxazine FAD ring and the Tyr398 and Tyr435 residues. There is an important hydrogen bond (1.98 Å) between the carbonyl moiety of Gln206 and the hydrogen atom of the amino group of the thiocarbomyl moiety. The hydroxy group of Tyr326 residue is in close contact (3.84 Å) with the N2 atom of pyrazole ring.

Docking of (−)-*S*-thiocarbomyl-3-(4-methylphenyl)-5-(4-chlorophenyl)-4,5-dihydro-(1H)-pyrazole, (compound **12**), which is the most potent competitive MAO B inhibitor of those in this study, showed none of the phenyl rings to be exactly oriented between Tyr398 and Tyr435 residues. The chloride atom of chlorophenyl ring is positioned between the two hydroxyl side chains, Tyr398 and Tyr435, forming two electrostatic interactions (at a distance of 4.90 Å between Cl and HO-Tyr398 and a distance of 3.30 Å between Cl and HO-Tyr435). The other interactions contributing to the binding of this inhibitor are between: N1 (pyrazole ring) and H_2N-Gln206 (4.32 Å), N2 (pyrazole ring) and HO-Tyr326 (4.18 Å), thiocarbamoyl N and HO-Tyr326 (2.17 Å), thiocarbamoyl NH_2 and HO-Tyr326 (2.26 Å), thiocarbamoyl NH_2 and H_2N-Gln206 (2.32 Å), and thiocarbamoyl C=S and H_2N-Gln206 (4.27 Å).

Discussion

In addition to the binding modes and three dimensional pictures of inhibitors in the active site, the result of these docking studies allowed the binding free energy (ΔG_b) and inhibition constants (K_i) to be estimated for each inhibitor. These are essential requirements for structure-based drug design and high throughput drug screening. The objective of this study was to implement a robust, working simulation program in order to calculate the above mentioned properties of experimentally tested reversible MAO-B inhibitors and compare these *in silico* results with those obtained experimentally. The high-resolution crystal structure (1S3E, 1.6 Å) of recombinant purified human MAO-B was used in the AutoDock 3.05 program, with necessary modifications made by GROMACS molecular dynamics simulation program and the AutoDock ADDSOL utility program.

Experimental inhibition constants were from different literature sources (see Table 2). Since these were for MAO-B from different sources (bovine-liver for compounds **1**, **2**, **3**, bovine-brain for **11** and **12**, human liver for **5** and **7**, and rat brain for **4**, **6**, **8**, **9** and **10**), we did not expect to obtain exact experimental values by computational calculations. Differences between experimental and computational results may also arise in the approximations and simplifications made during the computation process; for example, no explicit water molecules were considered during docking simulation. Furthermore, AutoDock 3.05 uses empirical scoring function for free energy calculations. Considering all these factors, a very reasonable prediction of inhibition constants was obtained, which were at least in the correct order of magnitude.

As seen from Table 2, where experimental inhibition constants are in descending order, inhibition constant values of the first six compounds (**1**–**7**) are in the micromolar range and the last six (**8**–**12**) are in the nanomolar range. In order to evaluate the accuracy of the docking, the experimental K_i values were compared to those obtained computationally. Excellent agreement was obtained in the case of compounds **6**, **7**, **9**, **10**, **11** and **12** (differences <6 fold), reasonable prediction of inhibition constants was obtained for compounds **2**, **4**, **5** and **8** (differences <10 fold), and an acceptable estimation of inhibition constants was obtained for compounds **1** and **3** (differences 12.5, and 10.3 fold, respectively). Compounds **11** and **12** were also docked using a different program, the GLUE flexible docking program, by Manna et al. (2002). They obtained K_i values of 2.21 nM for **11** and 5.14 nM for **12**, agreeing very well with our results (5.04 nM and 2.74 nM, respectively).

In conclusion, the data obtained by the AutoDock studies allowed us to estimate the free energies of binding, binding modes, and inhibition constants and provide a promising tool for the discovery of new, potent inhibitors for use as pharmacological agents. The AutoDock methodology will be useful in the rational designing and screening of novel selective potent MAO-B inhibitors.

Acknowledgements

We would like to acknowledge Özge Yelekçi for arrangements of Figures and Kadir Has University for providing us its computational facility to this study.

References

Bach AWJ, Lan NC, Johnson DL, Abell CW, Bembenek ME, Kwan SW, Seeburg PH, Shih JC (1998) cDNA cloning of human liver monoamine oxidase A and B: molecular basis of differences in enzymatic properties. Proc Natl Acad Sci USA 85: 4934–4938

Berendsen HJC, van der Spoel D, van Drunen R (1995) GROMACS: a message-passing parallel molecular dynamics implementation. Comp Phys Comm 91: 43–56

Binda C, Vinson PN, Hubalek F, Edmondson DE, Mattevi A (2002) Structure of human monoamine oxidase B, a drug target foe the treatment of neurological disorders. Nat Struct Biol 9: 22–26

Binda C, Hubalek F, Li M, Edmondson DE, Mattevi A (2004) Crystal structure of human monoamine oxidase B, a drug target enzyme monotopically inserted into the mitochondrial outer membrane. FEBS Lett 564: 225–228

Binda C, Hubalek F, Li M, Herzig Y, Sterling J, Edmondson DE, Mattevi A (2004) Crystal Structure of monoamine oxidase B in complex with four inhibitors of the N-propargylaminoindane class. J Med Chem 47: 1767–1774

Carotti A, Carrieri A, Chimichi S, Boccalini B, Cosimelli B, Gnerre C, Carotti A, Carrupt PA, Tesla B (2002) Natural and synthetic geiparvarins are strong and selective MAO-B inhibitors. Synthesis and SAR Studies. Bioorg Med Chem Lett 12: 3551–3555

Carrieri A, Carotti A, Barreca LM, Altomare C (2002) Binding models of reversible inhibitors to type-B monoamine oxidase. J Comput Aided Mol Des 16: 769–778

Cesura AM, Gottowik J, Lahm HW, Lang G, Imhof R, Malherbe P, Röthlisberger U, Da Prada M (1996) Investigation on the structure of the active site of monoamine oxidase-B by affinity labeling with the selective inhibitor lazabemide and by site-directed mutagenesis. Eur J Biochem 236: 996–1002

Chimenti F, Maccioni E, Secci D, Bolasco A, Chimenti P, Granese A, Befani O, Turini P, Alcaro S, Ortuso F, Cirilli R, La Torre F, Cardia MC, Distinto S (2005) Synthesis, molecular modeling studies, and selective inhibitory activity against monoamine oxidase of 1-thiocarbamoyl-3,5-diaryl-4,5-dihydro-(1H)-pyrazole derivatives. J Med Chem 48: 7113–7122

De Colibus L, Min L, Binda C, Lustig A, Edmondson DE, Mattevi A (2005) Three-dimentional structure of human monoamine oxidase A: relation to the structure of rat MAO A and human MAO B. Proc Natl Acad Sci USA 102: 12684–12689

Edmondson DE, Bhattacharrya AK, Xu J (2000) Evidence for alternative binding modes in the interaction of benzylamine analogues with bovine liver monoamine oxidase B. Biochim Biophys Acta 1479: 52–58

Erdem SS, Yelekci K (2001) Computer modeling of oxygen containing heptylamines as monoamine oxidase inactivators. J Mol Str (Theochem) 572: 97–106

Erdem SS, Karahan O, Yildiz I, Yelekci K (2006) A computational study on the amine-oxidation mechanism of monoamine oxidase: insight into the polar nucleophilic mechanism. J Bio Org Chem 4: 664–658

Gasteiger J, Marsili M (1980) Iterative partial equalization of orbital electronegativity – a rapid access to atomic charges. Tetrahedron 36: 3219–3228

Hubalek F, Binda C, Li M, Herzig Y, Sterling J, Youdim MBH, Edmondson DE (2004) Inactivation of purified human recombinant monoamine oxidase A and B by rasagiline and its analogues. J Med Chem 47: 760–1766

Hubalek F, Binda C, Khalil A, Li M, Mattevi A, Castagnoli N, Edmondson DE (2005) Demonstration of isoleucine 199 as a structural determinant for the selective inhibition of human monoamine oxidase B by specific reversible inhibitors. J Biol Chem 280: 15761–15766

Humphrey W, Dalke A, Schulten K (1996) VMD – Visual Molecular Dynamics. J Molec Graphics 14: 33–38. http://www.ks.uiuc.edu/Research/vmd

Lebreton L, Curet O, Gueddari S, Mazouz F, Bernard S, Burstein C, Milcent R (1995) Selective and potent monoamine oxidase type B inhibitors: 2-substituted 5-aryltetrazole derivatives. J Med Chem 38: 4786–4792

Li M, Binda C, Mattevi A, Edmondson DE (2006) Functional role of the ''aromatic cage'' in human monoamine oxidase B: structures and catalytic properties of Tyr435 mutant proteins. Biochemistry 45: 4775–4784

Lindahl E, Hess B, van der Spoel D (2001) Gromacs 3.0: a package for molecular simulation and trajectory analysis. J Mol Mod 7: 306–317

Manna F, Chimenti F, Bolasco A, Secci D, Bizzarri B, Befani O, Turini P, Mondovi B, Alcaro S, Tafi A (2002) Inhibition of amine oxidases activity by 1-acetyl-3,5-diphenyl-4,5-dihydro-(1H)-pyrazole derivatives. Bioorg Med Chem Lett 12(24): 3629–3633

Mazouz F, Lebreton L, Milcent R, Burstein C (1990) 5-Aryl-1,3,4-oxadiazol-2(3H)-one derivatives and sulfur analog as new selective and competitive monoamine oxidase type B inhibitors. Eur J Med Chem 25: 659–671

Morris GM, Goodsell DS, Halliday RS, Huey R, Hart WE, Belew RK, Olson AJ (1998) Automated docking using a Lamarckian genetic algorithm and empirical binding free energy function. J Comp Chem 19: 1639–1662

Morris GM, Goodshell DS, Huey R, Hart WE, Halliday RS, Belew RK, Olson AJ (1999) *Autodock (version 3.05)*, Molecular Graphics Laboratory, Department of Molecular Biology, The Scripps Research Institutes, http://www.scripps.edu/pub/olson-web/doc/Autodock/), La Jolla, CA, USA

Pare CM (1976) Unwanted effects of long-term medication in schizophrenia and depression. Pharmakopsychiatr Neuropsychopharmakol 9: 187–192

Pedretti A, Villa L, Vistoli G (2004) Vega – an open platform to develop chemo-bio-informatics applications, using plug-in architecture and script programming. J Comput Aided Mol Des 18: 167–173

Shih J, Chen K, Ridd MJ (1999) Monoamine oxidase: from genes to behaviour. Annu Rev Neurosci 22: 197–217

Silverman RB, Lu X, Zhou JJP, Swihart A (1994) Monoamine oxidase B-catalyzed oxidation of cinnamylamine-2,3-oxide; further evidence against a nucleophilic mechanism. J Am Chem Soc 116: 11590–11591

Silverman RB, Lu X, Blomquist G, Ding CZ, Yang S (1997) Inactivation of monoamine oxidase B by benzyl 1-(aminomethyl)cyclopropane-1-carboxylate. Bioorg Med Chem 5: 297–304

Tetrud JW, Langston JM (1989) The effect of deprenyl (selegiline) on the natural history of Parkinson's disease. Science 245: 519–522

Toprakçi M, Yelekci K (2005) Docking studies on Monoamine Oxidase-B inhibitors: estimation of inhibition constants (K_i) of a series of experimentally tested compounds. Bioorg Med Chem Lett 15: 4438–4446

Veselovsky AV, Ivanov AS, Medvedev AE (2004) Computer modelling and visualization of active site of monoamine oxidases. Neuro Toxicology 25: 37–46

Wavefunction, Inc. 18401 von Karman Avenue, Suite 370, Spartan'02, Irvine, CA 92612, USA

Youdim MBH, Maruyama W, Naoi M, Youdim, MBH (2005) Neuropharmacological, neuroprotective and amyloid precursor processing properties of selective MAO-B inhibitor antiparkinsonian drug, rasagiline. Drugs Today (Barc) 41: 369–391

Youdim MBH, Edmondson DE, Tipton KF (2006) The therapeutic potential of monoamine oxidase inhibitors. Nat Rev Neurosci 7: 295–309